The dielectric properties of random R - C networks as an explanation of the `universal' power law dielectric response of solids

1999 J. Phys.: Condens. Matter 11 9081

(http://iopscience.iop.org/0953-8984/11/46/310)

J. Phys.: Condens. Matter **11** (1999) 9081–9093. Printed in the UK PII: S0953-8984(99)06821-6

The dielectric properties of random *R–C* networks as an explanation of the 'universal' power law dielectric response of solids

D P Almond† and B Vainas‡

† Department of Materials Science and Engineering, University of Bath, Bath BA2 7AY, UK
‡ Soreq Research Center, Yavne 81800, Israel

Received 11 August 1999

Abstract. Simulations of the AC electrical characteristics of 2D square networks randomly filled with resistors or capacitors exhibit many features in common with experimental dielectric responses of solids. These include the 'universal' fractional power law dispersions in permittivity and dielectric loss characterized by the Cole–Davidson response function. Simulations are presented of networks containing different proportions of resistors and capacitors which show that the power law frequency response is accounted for well by the logarithmic mixing rule. Limiting high and low frequency characteristics are found to be controlled by percolation paths of either resistors or capacitors. It is suggested that the power law response of a solid could be an indication that it is microscopically inhomogenous, containing an effective microscopic random network of conducting and dielectric insulating islands.

1. Introduction

The dielectric properties of solids across the radio frequency range (∼1 Hz to ∼10 MHz) have long been attributed to the contributions of microscopic dipolar, or dipolar-like, components to the total dielectric response. The basis of the most commonly used theoretical interpretation of the phenomena is Debye's model [1] which was devised to explain the dielectric response of viscous liquids containing freely floating dipoles. This model predicted the complex dipole permittivity, $\varepsilon^*(\omega)$, to be the following simple function of the parameter $\omega\tau$:

$$\varepsilon^*(\omega) = \varepsilon'(\omega) + \mathrm{i}\varepsilon''(\omega) = \frac{\Delta\varepsilon}{1 + \mathrm{i}\omega\tau} = \frac{\Delta\varepsilon}{1 + \omega^2\tau^2} - \mathrm{i}\frac{\Delta\varepsilon\omega\tau}{1 + \omega^2\tau^2} \tag{1}$$

in which $\omega\tau$ is the product of measurement angular frequency and a characteristic dipole relaxation time and $\Delta\varepsilon = \varepsilon(0) - \varepsilon_\infty$ is the difference between the static permittivity and that at an 'infinitely high' frequency, far exceeding the response rates of the dipoles. The $\omega\tau$ dependence of the real and imaginary components of permittivity are shown, plotted logarithmically, in figure 1(a). At low frequency ($\omega\tau \ll 1$) dipole relaxation rate, τ^{-1}, far exceeds the applied frequency and a full dipolar contribution to permittivity is predicted. At high frequency ($\omega\tau \gg 1$) the applied frequency far exceeds dipole relaxation rate and dipoles are unable to respond rapidly enough to contribute to permittivity, resulting in the high frequency decrease in dipolar permittivity. At intermediate frequencies ($\omega\tau \sim 1$) there is a partial contribution to the real part of the permittivity and a characteristic peak in the imaginary, dielectric loss, part. The latter peaks at $\omega\tau = 1$, providing the well known and widely used

0953-8984/99/469081+13$30.00

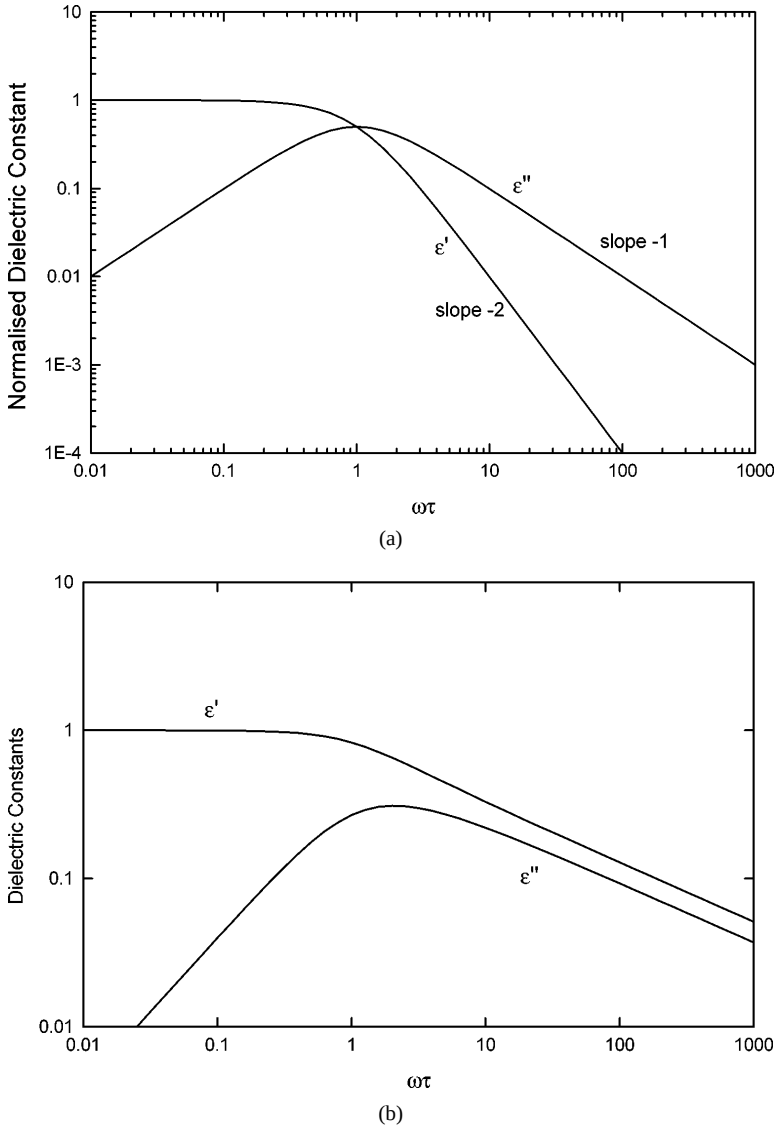

Figure 1. (a) The Debye dielectric response function, equation (1), and (b) the Cole–Davidson dielectric response function, equation (3) for $\beta = 0.4$, plotted logarithmically against $\omega\tau$.

means of assessing dipole relaxation time, τ, by locating the frequency at which dielectric loss peaks.

In the classical Debye theory the relaxation time, τ, arises from the retarding effect that the viscosity of a liquid has on the rotation of a floating dipole. A similar term is necessary to account for dipolar response in a solid where dipoles are taken to respond to an applied electric field by rotation between a series of allowed orientations that are separated by activation energy barriers. Dipolar rotation is considered to be a thermally activated process and dipole relaxation time is expected to vary with temperature as:

$$\tau = \tau_0 \exp(E_A/kT) \tag{2}$$

where E_A is the activation energy, k is the Boltzmann constant and τ_0 is the inverse of the 'attempt frequency' for a dipole confined in a potential well of depth E_A. Hence the activation energy for a dipolar rotation may be obtained by an Arrhenius analysis of the temperature dependence of relaxation times, determined from dielectric loss measurements. It is well known that dielectric measurements of solids have been extensively exploited in this way. However, it is also well known that the actual dielectric response of the majority of solids is only broadly similar to that indicated by equation (1) and shown in figure 1(a). Whilst permittivity is a decreasing function of frequency and dielectric loss passes through a peak, the functional forms of these frequency dependences seldom match the Debye expressions. Dielectric loss peaks are usually found to be far broader in frequency than predicted by Debye and the high frequency ($\omega\tau \gg 1$) tails of both permittivity and dielectric loss are found to decay as a power of frequency ($\propto \omega^{-n}$ with $0 < n < 1$). Davidson and Cole [2] suggested an empirical modification to the Debye expression which has been found to provide a better representation of experimental data obtained from dielectric solids:

$$\varepsilon^*(\omega) \propto \frac{1}{(1 + \mathrm{i}\omega\tau)^{\beta}} \tag{3}$$

in which $0 < \beta < 1$. An example of the of the $\omega\tau$ dependences of permittivity and dielectric loss modelled by the Cole–Davidson function is shown in figure 1(b), for comparison with the Debye expression, figure 1(a). The principal difference is that the Cole–Davidson expression reproduces the widely observed common power law decay of permittivity and dielectric loss whilst the original Debye expression has them decaying with frequency as ω^{-2} and ω^{-1}, respectively.

There have been a very large number of theoretical explanations of the experimentally observed 'universal' dielectric response, references to many of which can be found in reviews [3] and [4] by Jonscher. The majority of these explanations can be divided into two classes: Debye relaxation models with distributions of relaxation times (DRT) and models employing fundamentally modified atomic level relaxation processes [5–7]. It is well known [8, 9] that the DRT approach can be used successfully to model data and that this merely transforms the problem from explaining a universal frequency dependence to explaining a universal relaxation time or activation energy distribution for dipole rotation or other dielectric relaxation processes. We believe that a major objection to the modified relaxation processes, atomic level, models is the ubiquity of the observed dielectric response phenomena. This ubiquity extends across relaxation species, covering dielectric phenomena attributable to electronic, atomic, ionic, molecular and macro-molecular relaxation. The characteristic response is found in all classes of materials, including: single crystals, polycrystalline samples, glasses, polymers, composites and semiconductors. Very similar response phenomena are also found in measurements obtained by a range of other techniques, such as: mechanical relaxation; viscoelasticity; AC conductivity; electrical noise and NMR. It is natural to seek a common explanation for all the phenomena and the modified relaxation process models seem to be far too specific to a particular class of material, a particular phenomenon or a particular scale of relaxation.

There is a long tradition of modelling the electrical responses of solids by combinations of resistors and capacitors. Early workers [10–12] introduced a number of parallel coupled *R–C* circuit elements coupled in series to represent multiple phases or the effects of grain boundary interfaces. However, because these provided a poor representation of the experimental data, progressively more complex arrays of *R–C* elements have been utilized. Coverdale *et al* [13] have developed large networks of components using materials microstructures to determine component values and connections. Work such as this has been more successful in reproducing observed electrical response characteristics but it has failed to clarify the physical origins of the power laws.

The purpose of this paper is to draw attention to the similarity between the dielectric responses of a large random networks of resistors and capacitors and the near universal dielectric response of solids that has been outlined above. This similarity leads to the possibility that many of the samples that have been examined using dielectric measurements were inhomogenous with internal regions of both insulating dielectric and electrically conducting material arranged as a microscopic random network.

2. The AC electrical response of a random *R–C* network

Truong and Teran [14] provided both experimental and theoretical evidence to support the suggestion that the dielectric properties of a solid might be closely linked to those of a random *R–C* network. They found the high frequency dielectric permittivity and dielectric loss of conducting polymers to exhibit power law dispersions similar to those arising from the Cole–Davidson expression, equation (3) shown in figure 1(b). These polymers contained a network of macroscopic conducting particles introduced into an insulating polymer matrix. It was argued that a suitable representation was a randomly connected network of resistors and capacitors. The randomness of the connections ensures that locally within the sample it is equally likely to find components connected in series as in parallel. For such a network, the macroscopic impedance or admittance may be estimated by the logarithmic mixing rule [15]:

$$\ln \sigma^* = \sum_n \alpha_n \ln \sigma_n^*$$
$$\sigma^* = \prod_n (\sigma_n^*)^{\alpha_n} \tag{4}$$

in which σ^* is the measured complex conductivity of the network, σ_n^* and α_n are the complex conductivity and volume fraction of the nth component, respectively. The plausibility of this formula [15, 16] is indicated by noting that the equivalent formula for components all connected in parallel is:

$$(\sigma^*)^\nu = \sum \alpha_n (\sigma_n^*)^\nu \qquad \text{with } \nu = +1$$

whilst that for series connected components is

$$(\sigma^*)^\nu = \sum \alpha_n (\sigma_n^*)^\nu \qquad \text{with } \nu = -1$$

then the appropriate formula, equation (4), for randomly series–parallel connected components is obtained if $\nu \to 0$, noting $\sum \alpha_n = 1$.

Alternatively, for a binary system, the formula can be obtained from the need for invariance under the interchange of conductivities and volume fractions [17, 18] and in the case of equal proportions of the two component phases the formula has been shown to be rigorously exact [19]. The logarithmic mixing rule for the two component system is also known as Lichtenecker's rule [20] which has recently been revived in the evaluation of the dielectric response of a binary system [21].

The importance of the logarithmic mixing rule here is that it leads to power law frequency dependences of permittivity and dielectric loss of the types obtained from the Cole–Davidson expression, equation (3), at high frequencies. If it is postulated that a dielectric is composed of a random microscopic network of purely dielectric and purely conductive material, of permittivity ε and conductivity σ, respectively,

$$\sigma^*(\omega) = (\mathrm{i}\omega\varepsilon\varepsilon_0)^\alpha \sigma^{1-\alpha} \propto (\mathrm{i}\omega)^\alpha$$
$$\varepsilon^*(\omega) = \sigma^*(\omega)/\mathrm{i}\omega\varepsilon_0 \propto (\mathrm{i}\omega)^{\alpha-1} \tag{5}$$

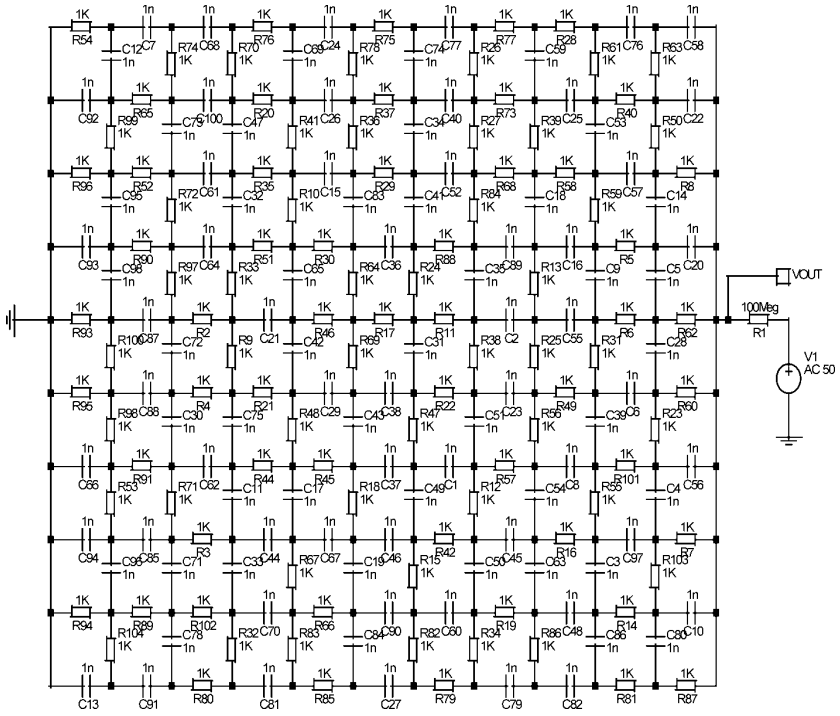

Figure 2. A SIMetrix network of 200 randomly placed resistors and capacitors and the external circuit used to obtain AC response characteristics.

which is of the same form as the power law term arising from equation (3) for $\omega\tau \gg 1$ shown in figure 1(b). The interpretation of the power law exponent, α, is that it represents the proportion of the material that is purely capacitive. This interpretation was advanced by Truong and Teran [14] to explain the AC response of their conducting polymers.

3. Random *R–C* network simulations

Work on the AC electrical characteristics of random *R–C* networks was reviewed by Clerc *et al* [18]. Much of this has concentrated on developing an understanding of networks with compositions that are close to the percolation threshold. In this work we are concerned with more general compositions that provide an overall capacitive response but which include a smaller proportion resistive components.

Simulations were performed using commercial SIMetrix [22] software which employs simulation algorithms from SPICE version 3f.5. Typically, simulations of network response were obtained across the frequency range 1 Hz to 1 GHz at ten points in each decade of the frequency spectrum. An example of a 2D square network randomly filled with resistors and capacitors, to be referred to below as a 'random *R–C* network' for brevity, is shown in figure 2. This network which contains only 200 components is reproduced here as an illustration of the type of network that has been analysed. The networks used for the majority of the simulations contained 512 components, 1 kΩ resistors or 1 nF capacitors in a specified proportion, randomly placed in the network. Results of simulations from networks containing significantly fewer (170) and significantly larger (2024) numbers of components were found to differ little and to exhibit the same principal characteristics, discussed below, that are the subject of this work.

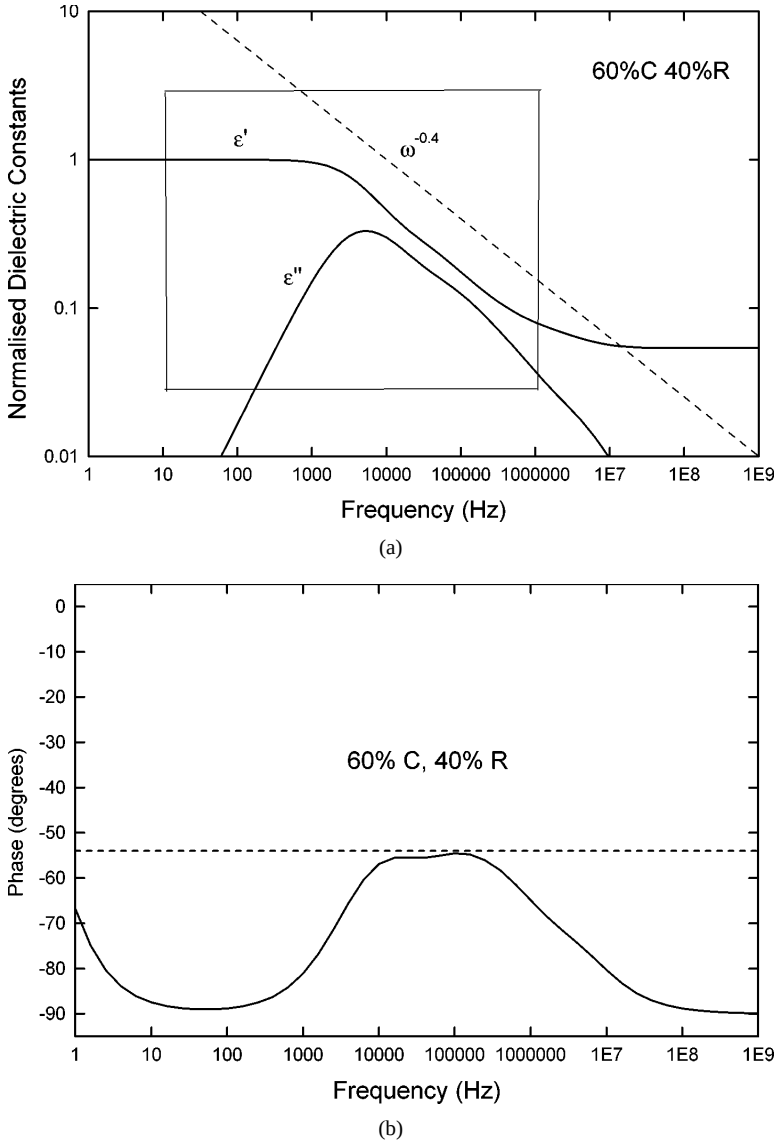

Figure 3. (a) The effective permittivity and dielectric loss of a random network of 512 components of which 60% were 1 nF capacitors and 40% were 1 kΩ resistors. (b) The phase–frequency dependence of the voltage developed across the network. The dashed lines shows the logarithmic mixing formula, equation (5), prediction for the network. (c) A comparison of the frequency dependences of the AC conductances of a 1 nF capacitor and a 1 kΩ resistor.

The effects of network size are considered in more detail below. The 100 MΩ external resistor, figure 2, was placed in series with the AC voltage source to provide a constant AC current source. The earth and V_{out} line represent the electrodes on the two sides of a sample. It was found that large networks of predominantly capacitive components contained a number of 'floating nodes' which prevented the simulation programme from establishing a full set of DC potentials—an essential step prior to the running of the AC simulation. To overcome this each 1 nF capacitor was shunted by a 1 GΩ resistor (not shown in figure 2). This eliminated the

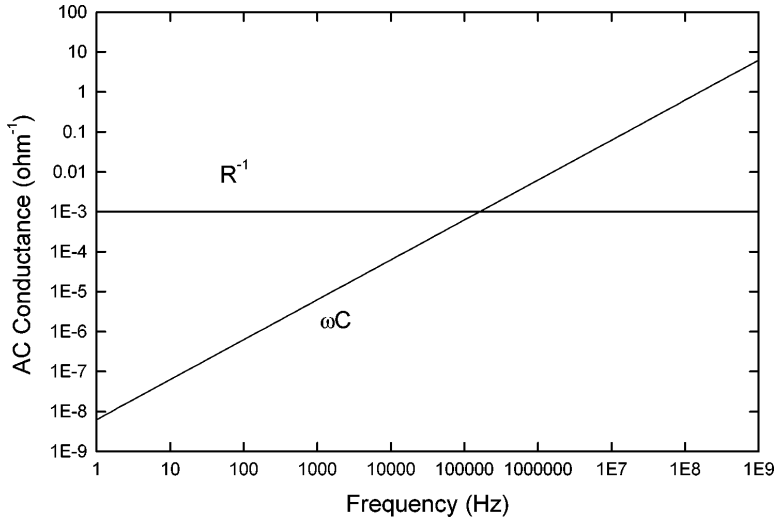

(c)

Figure 3. (Continued)

DC floating node problem and introduced a negligible effect on the network AC response at frequencies above about 10 Hz.

3.1. Simulation of a 'dielectric' 60% C 40% R random network

Simulation results of a random network in which 60% of the components were 1 nF capacitors and the remainder were 1 kΩ resistors are shown in figure 3(a) in the form of the effective normalized dielectric constants, ε' and ε'', of the network against frequency. It is evident that these network characteristics are similar to the familiar dielectric characteristics of solids shown in figure 1. The frequency dependence of the phase of the voltage V_{out} across the network is shown in figure 3(b). At high and low frequencies this is $\sim -90^\circ$, corresponding to the high and low frequency plateaux in ε' where the network behaves as an almost purely capacitive element. At intermediate frequencies, however, the phase rises and is approximately constant between $\sim$10 kHz and 1 MHz. Across the same frequency range ε' and ε'' decline with frequency in a power law fashion, of the type exhibited by the Cole–Davidson function, figure 1(b). In this intermediate frequency range the electrical response of the network is close to that, equation (5), obtained from the logarithmic mixing rule. In this network, where 60% of the components are capacitors, $\alpha = 0.6$ and equation (5) indicates a phase $= -54^\circ$ and both ε' and $\varepsilon'' \propto \omega^{-0.4}$. It can be seen that the simulation data, figures 3(a) and 3(b), are in good agreement with these expectations in the intermediate frequency range. An appreciation of how the capacitive and resistive components of AC conductance within the network vary with frequency, shown in figure 3(c), leads to an understanding of the origins of the almost purely capacitive characteristics at high and low frequencies. At high frequencies the capacitive component conductance $\omega C \gg R^{-1}$, the resistive component conductance, and the resistive network links are effective open circuits. The AC current becomes confined to a percolation 'backbone' of capacitors between the 'electrodes'. The percolation threshold for a 2D square network occurs for a concentration of 50% of links occupied by a particular type of conductor. In this case of 60% capacitors there should be a well established percolation backbone of capacitors linking

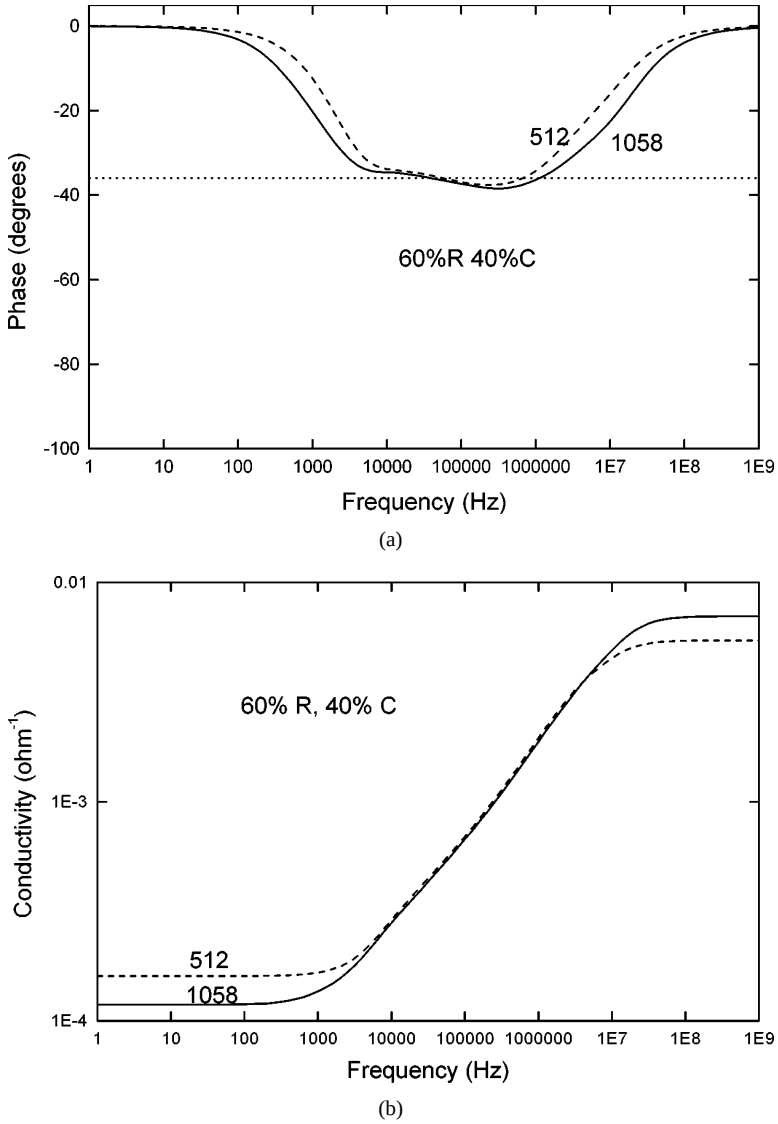

Figure 4. (a) The phase–frequency dependence of the voltage developed across random networks of 512 (dashed) and 1058 (solid) components of which 60% were 1 kΩ resistors and 40% were 1 nF capacitors. The dotted line shows the logarithmic mixing formula, equation (5), prediction for the networks. (b) The frequency dependence of the AC conductivities of the networks. (c) The effective permittivity and dielectric loss of the 512 component network.

the electrodes. The magnitude of the high frequency plateau capacitance, $\propto \varepsilon'$, is that of the capacitors in the percolation backbone alone, as the resistive links may be taken to be open circuits. At low frequencies $\omega C \ll R^{-1}$ and the resistive links act as effective short circuits. However, as only 40% of the components are resistive, a complete percolation path of resistors will not be found between the electrodes. The AC conduction is still dependent on a capacitive path between the electrodes. This will consist of the percolation backbone with many additional capacitors being apparently added in parallel to it by the resistive links, which at low frequencies act as short circuits. Consequently, the magnitude of ε' on the low frequency plateau exceeds

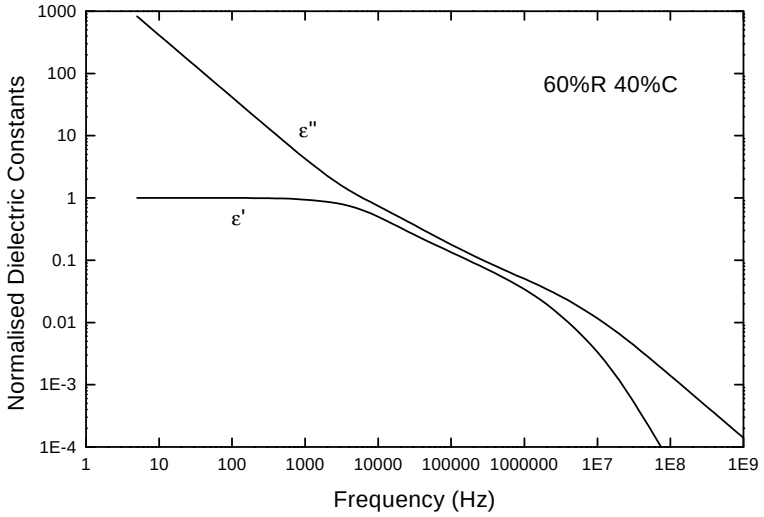

(c)

Figure 4. (Continued)

that on the high frequency plateau. At intermediate frequencies, $\omega C \sim R^{-1}$, the random series–parallel network, logarithmic mixing rule, AC response is produced, as discussed above.

3.2. Simulation of a 'conductive' 60% R 40% C random network

If the proportions of the network components are reversed so that 60% are resistors, the network response becomes predominantly conductive. A 2D square network was randomly filled with a total of 512 components comprising 1 kΩ resistors and 1 nF capacitors, numerically in the ratio 6:4. The simulation frequency dependences of: the phase of the AC voltage across the network; the network AC conductivity and the effective network dielectric constants are shown in figures 4(a)–(c).

In contrast to the phase of the dielectric network, figure 3(b), the phase of the conductive network, figure 4(a), $\sim 0^\circ$ at high and low frequencies, corresponding to the high and low frequency plateaux in AC conductivity, figure 4(b). Since the network percolation threshold of 50% is exceeded by the proportion of resistors in the network, a well developed percolation backbone of resistors will be present in the network to carry currents between the 'electrodes', earth and V_{out}. At low frequencies the AC conductances of the capacitors are so low, figure 3(c), that the capacitors may be regarded as being open circuits and the network AC conductivity is that of the percolation backbone alone. At high frequencies the reverse is true, figure 3(c), and the capacitors act as short circuit links that effectively add further resistors in parallel to the percolation backbone and raise the AC conductivity to the high frequency plateau level, figure 4(b). At intermediate frequencies, where the AC conductances of the resistors and capacitors are comparable, the phase approximates the logarithmic mixing rule value of -36°, obtained from setting α in equation (5) $= 0.4$ as in this network only 40% of the components are capacitors. Over the same frequency range the AC conductivity increases with frequency in a power law fashion, equation (5), as $\sim \propto \omega^{0.4}$. The AC conductivity simulation results, figure 4(b), mirror the permittivity simulations shown in figure 3(a). The dielectric representation of the 60% R 40% C network simulation data, figure 4(c), exhibits a

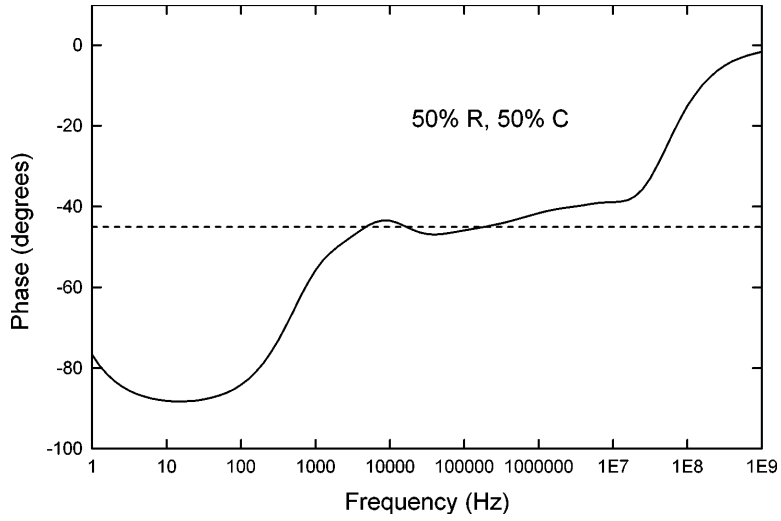

(a)

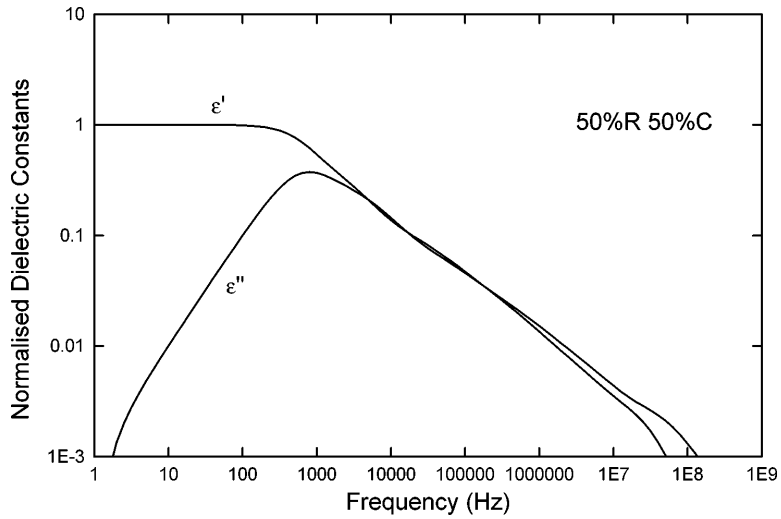

(b)

Figure 5. (a) The phase–frequency dependence of the voltage developed across a random network of 512 components of which 50% were 1 kΩ resistors and 50% were 1 nF capacitors. The dashed line shows the logarithmic mixing formula, equation (5), prediction for the network. (b) The effective permittivity and dielectric loss of the network.

Cole–Davidson-like permittivity, ε', component but no peak in the dielectric loss, ε'', due to the non-zero DC conductivity of the conductive network. However, the intermediate frequency response retains the characteristic common power law decay of both ε' and ε'' as $\sim \propto \omega^{-0.6}$, predicted by equation (5).

3.3. Simulation of a percolation threshold 50% R 50% C random network

As was mentioned above, the characteristics of random *R–C* networks at the percolation threshold have been investigated in some depth [18]. For completeness, the results of a

simulation of a network with the percolation threshold composition of 50% R and 50% C are presented here in figure 5. In this network there were no percolation backbones of either resistors or capacitors between the electrodes. The phase of the network output voltage, shown in figure 5(a), is $\sim -90^\circ$ at low frequencies, dominated by the high impedances of the capacitors along the path between the electrodes. At high frequencies the phase $\sim 0^\circ$, dominated by the relatively high impedances of the resistors along the path between the electrodes. At intermediate frequencies the phase takes the value $\sim 45^\circ$, expected from the logarithmic mixing rule where $\alpha = 0.5$. The dielectric constants shown in figure 5(b) exhibit a Cole–Davidson-like characteristic with a $\sim \propto \omega^{-0.5}$ power law decay of both ε' and ε'' across the intermediate frequency range.

4. Discussion

There is a remarkable similarity between the dielectric response of the random network, figure 3(a), and the Cole–Davidson response, figure 1(b), that characterizes many dielectric data. This similarity becomes more pronounced where the random network simulation data is restricted to a frequency range typical of that covered by experimental data, the area within the box in figure 3(a). Consequently, we are led to suggest that a possible explanation of the Cole–Davidson form of dielectric response is that that materials which exhibit these characteristics are internally inhomogeneous, comprising what amounts to random networks of microscopic capacitive islands and electrically conductive links. The physical natures of the capacitive and conductive islands are, at this stage, largely a matter of conjecture. There is no problem in identifying such regions in composites, such as the conducting polymers discussed above, and in materials where conduction paths are known to develop due to the ingress of water or the development of inter-granular conductive phases. That such paths may be present in a wide range of dielectrics of all types is recognized to be contentious. The quantitative plausibility of this suggestion may be judged by considering the materials properties that govern the frequency range over which the characteristic power laws are observed. It has been shown that the power law dispersions occur in the intermediate frequency range where $\omega C \sim R^{-1}$ or, equivalently, where $\omega\varepsilon'\varepsilon_0 \sim \sigma$ in which ε' is the permittivity of the dielectric material in the insulating capacitive islands and σ is the electrical conductivity of the electrically 'leaky' regions. In a typical polar dielectric $\varepsilon' \sim 10$ and the condition becomes $\omega \sim 10^{10}\sigma$. Hence for a dielectric to exhibit a power law about a typical frequency of 10 kHz, the conductivities of the resistive regions $\sim 10^{-5}\ \Omega^{-1}\ \mathrm{m}^{-1}$. This magnitude of conductivity could arise from localized impurities or defects in a dielectric solid. It is over an order of magnitude lower than the room temperature intrinsic conductivity of the 1.1 eV energy gap semiconductor, silicon. In addition, it is likely that such a conductivity in a leaky dielectric would arise from thermal excitations which would lead to the conductivity having an Arrhenius temperature dependence. This, in turn, would cause the characteristic network frequency, $\omega_N = \sigma/\varepsilon'\varepsilon_0$, and consequently the dielectric loss peak frequency to have an Arrhenius temperature dependence. The latter, of course, is widely observed experimentally, as was mentioned in the introduction.

Alternatively, it is recognized that the Debye dielectric response, equation (1), can be modelled by a series R–C circuit, setting $\tau = RC$. Consequently, an inhomogenous dielectric containing a phase with a Debye-like dielectric response in a frequency independent dielectric matrix could be modelled as a random network of pure capacitors and circuits comprising a resistor and capacitor coupled in series, to simulate the Debye phase. The resulting response characteristics of such a network are essentially those of the random R–C networks presented here.

The AC electrical characteristics of the conductive network have much in common with those found experimentally in hopping ion conductors and weak electronic conductors.

A detailed comparison of conductive network simulation results and the AC electrical characteristics of ionic conductors has been presented elsewhere [23].

All the simulation data presented here were obtained from randomly filled 2D square *R–C* networks. The results of 3D network simulations are found to be qualitatively the same as those of 2D network simulations [13, 18]. Here differences between the results of 2D network simulations and the corresponding 3D network simulations are anticipated in the detail rather than the general form of the responses which should be retained. For example, the percolation threshold composition of a 3D square network, obtained by simulations, is 24.88% [24] whilst it is 50% for a 2D square network.

The frequency ranges of the power law dispersions in network permittivity and dielectric loss/AC conductivity obtained here are narrower than reported in some experimental studies of the properties of solids. The extent of the frequency range, over which the power law holds appears to be widest for the 50% *R* 50% *C* composition. This is similar to the results obtained by Clerc *et al* [18]. The extent of this power law has been found to be affected by the number of components in the simulation network. The effects of increasing the number of components from 512 to 1058 for the conductive 60% *R* 40% *C* network are shown in figures 4(a) and 4(b). Whilst the magnitude of the conductivity in the power law region in figure 4(b) is unaffected the low frequency plateau conductivity is reduced and the high frequency plateau conductivity is raised, resulting overall in an increase in the frequency range over which the power law AC conductivity component is evident. The decrease in the low frequency plateau conductivity is consistent with the increase in the side dimension of the square network (from 16 to 23 components) increasing the length and hence the net resistance of the percolation path between the electrodes that accounts for the low frequency plateau conductivity. The increase in the high frequency plateau conductivity arises from the increase in the number of resistive components that become attached to the percolation backbone at high frequencies due to the doubling of the number of components in the network. A similar increase in the extent of the power law regions of the dielectric network has also been obtained by increasing the network size. It seems clear that the extents of the power law regions are determined simply by the relative magnitudes of the mixing rule, power law conductivities of the networks as a whole and the conductivities of the percolation backbones that form between the electrodes at high and low frequencies. Work is in progress to clarify the effects of composition and size on the extent and location of the power law frequency region. We would anticipate similar behaviour with the size of three-dimensional random networks, with the difference that the magnitude of the mixing rule, power law conductivity should increase with the side dimension of the network.

Dyre [25] has shown for a different type of network that a broadening in the power law frequency range results from a distribution of effective component parameters, ε and σ. In a solid where σ is thermally activated, a subtle distribution in energy barriers, resulting from local energetic variations caused by defects or impurities, can lead to σ having a substantial range of values. This might then lead to the effective mixing of the responses of networks characterized by a similar wide range of ω_N values and an extension of the power law response frequency range.

5. Conclusions

The effective dielectric response of a 2D square network randomly filled with resistors or capacitors exhibits many characteristics that are very similar to the ‘universal dielectric responses’ of solids. We are led to suggest that the dielectric characteristic of solids are, in many cases, caused by the solid being internally inhomogeneous on a microscopic scale, being

effectively a random microscopic network of dielectric regions and regions that are electrically conducting. The 'universal power laws' arise naturally from this treatment with power law exponents related directly to the relative proportions of capacitive and conductive material in the dielectrics. The thermal activation of the dielectric loss peak frequency may be associated with that of the dielectric leakage rather than being attributed to a fundamental dipolar relaxation rate. It is perhaps an unfortunate coincidence that the Debye dielectric responses and those of random *R–C* networks are so similar. There are a few cases [26, 27] where genuine Debye responses have been measured in solids. We suggest that the key distinction of these is the very different form of the response on the high frequency side of the dielectric loss peak. Where the dielectric effects are caused by fundamental dipolar relaxation phenomena alone the permittivity, ε', and the dielectric loss, ε'', have the very different frequency dependences of ω^{-2} and ω^{-1}, whilst both have the same $\omega^{\alpha-1}$ frequency dependency where a random network of dielectric and conductive islands is involved. The random network model seems applicable to all classes of materials, possibly accounting for the ubiquity of the dielectric response of solids. It may also account for the anomalous power laws reported for other types of phenomenon.

References

[1] Debye P 1945 *Polar Molecules* (New York: Dover)
[2] Davidson D W and Cole R H 1951 *J. Chem. Phys.* **19** 1484
[3] Jonscher A K 1983 *Dielectric Relaxation in Solids* (London: Chelsea Dielectric)
[4] Jonscher A K 1996 *Universal Relaxation Law* (London: Chelsea Dielectric)
[5] Funke K 1993 *Prog. Solid State Chem.* **22** 111
[6] Ngai K L, Mundy J N and Jain H 1989 *Phys. Rev.* B **39** 6169
[7] Dissado L A and Hill R M 1984 *J. Chem. Soc. Faraday Trans.* **2** 291
[8] Wang J C and Bates J B 1992 *Solid State Ion.* **50** 75
[9] Macdonald J R 1987 *J. Appl. Phys.* **61** 700
[10] Bauerle J E 1969 *J. Phys. Chem. Solids* **30** 2657
[11] Beekmans N M and Heyne L 1976 *Electrochim. Acta* **21** 303
[12] Bruce P C and West A R 1983 *J. Electrochem. Soc.* **130** 662
[13] Coverdale R T, Jennings H M and Garboczi E J 1995 *Comput. Mater. Sci.* **3** 465
[14] Truong V T and Teran J G 1995 *Polymer* **36** 905
[15] Brown W F 1956 *Dielectrics (Handbuch der Physik 17)* (Berlin: Springer)
[16] McLachlan D S, Blaszkiewiez M and Newnham R E 1990 *J. Am. Ceram. Soc.* **73** 2187
[17] Reynolds J A and Hough J M 1957 *Proc. Phys. Soc.* B **70** 769
[18] Clerc J P, Giraud G, Laugier J M and Luck J M 1990 *Adv. Phys.* **39** 191
[19] Straley J P 1977 *Phys. Rev.* B **15** 5733
[20] Lichtenecker K 1926 *Z. Phys.* **27** 115
[21] Zakri T, Laurent J-P and Vauclin M 1998 *J. Phys. D: Appl. Phys.* **31** 15 889
[22] SIMetrix, Newbury Technology Ltd, Thatcham, Berks RG18 4LZ, UK
[23] Vainas B, Almond D P, Lou J and Stevens R 1999 *Solid State Ion.* **126** 65
[24] Gingold D B and Lobb C J 1990 *Phys. Rev.* B **42** 8220
[25] Dyre J C 1993 *Phys. Rev.* B **48** 12 511
[26] Deguchi K, Okaue E and Nakamura E 1982 *J. Phys. Soc. Japan* **51** 3569
[27] Fontanella J, Jones D L and Andeen C 1978 *Phys. Rev.* B **18** 4454